

P-glycoprotein Mediates Postoperative Peritoneal Adhesion Formation by Enhancing Phosphorylation of the Chloride Channel-3

Lulu Deng, Qin Li, Guixian Lin, Dan Huang, Xuxin Zeng, Xinwei Wang, Ping Li, Xiaobao Jin, Haifeng Zhang, Chunmei Li, Lixin Chen, Liwei Wang, Shulin Huang, Hongwei Shao, Bin Xu, Jianwen Mao

Supplemental Methods

Plasmids, Site-Directed Mutagenesis, and Transfection

The plasmid encoding a MDR1-GFP fusion protein was kindly provided by Prof. David Piwnicka-Worms[1]. Histone H3 ORF expression plasmids were purchased from OriGene Technologies, Inc. (RC219443, Rockville, MD, USA). The plasmids expressing Smad 2 and Smad 3 were purchased from Addgene, Inc. (plasmids 14930 and 11742, respectively, Addgene, Cambridge, MA). Flag-tagged CIC-3 (EX-E0037-M46) and cytokeratin 18 (EX-D0093-M98) constructs were purchased from GeneCopoeia (Guangzhou, China). Tyrosine residues Y342 were mutated to phenylalanine by site-directed mutagenesis with the Flag-CIC-3 fusion vector by GeneCopoeia. The entire coding sequence of each mutant was confirmed by sequencing. Vectors were transfected into cells by Xtreme gene HP reagent (Roche, Indianapolis, IN) following the manufacturer's instructions. At 48 h after transfection, cells were collected for immunoprecipitation and luciferase assays as described below.

Histone H3 Acetylation Assay

The proportion of acetylated histones H3 was assayed using the EpiQuick global histone H3 acetylation assay kit (Epigentek, P-4008-48) following the manufacturer's instructions. Briefly, histone proteins were stably spotted on strip wells. The acetylated histone H3 was recognized with high-affinity antibodies. The amount of acetylated H3 was quantified through an HRP-conjugated secondary antibody-color development system, and the absorbance at 450 nm was read in an automated microplate reader (type Elx800, Bio-Tek Instruments, Winooski,

USA). The amount of acetylated histone H3 in the total histone protein was calculated using the following formula: Acetylation % = OD (treated sample – blank) / OD (untreated control – blank) × 100%.

RNA Interference

Cultured peritoneal fibroblasts were transfected with stealth MDR1 siRNA (5'-GGAAAAGAAACCAACUGUC-3'; 5'-GACAGUUGGUUCUUUCC-3'), Stealth Smad 2 siRNA (5'-AUUCUUACCCUUGGUAAGATT-3'; 5'-UCUUACCAAGGGUAAGAAUTT-3'), Smad 3 siRNA (5'-GAUCGAGCUACACCUGAAUTT-3'; 5'-AUUCAGGUGUAGCUCGAUCTT-3') or the NC (negative control) siRNA (GenePharma) with the HiPerFect transfection reagent (Qiagen, Valencia, CA).

For si-MDR1 transfection *in vivo*, the stability and the silencing efficiency were improved through the addition of four phosphorothioate modifications at the 3' end, two phosphorothioate modifications at the 5' end, a 2'-methoxy (2'-OMe) modification, and a 3'-cholesterol conjugation (GenePharma.Co., Ltd, Shanghai, China). The modified siRNAs were complexed with *in vivo*-jetPEI (PolyPlus-transfection, Illkirch, France) according to the manufacturer's protocol and intraperitoneally injected every two days for two weeks. Briefly, for each rat (80-100g), 10 ml of *in vivo*-jetPEI were mixed with 50 µg of nucleic acids for an N:P ratio of 10:1 (10 nitrogen residues of jetPEI per phosphate in DNA) in a volume of 250 µl of 5% glucose solution. The mixture was incubated for 15 min. We confirmed the knockdown of P-gp by immunohistochemical analysis of colon tissues.

To identify the cultured cells with knockdown of MDR1 expression, the vector pGPU6/GFP-MDR1 shRNA was constructed with the same sequence as the siRNA for MDR1 (GenePharma.Co., Ltd, Shanghai, China). A control vector was also constructed containing a non-silencing scrambled sequence (shNC). Vectors were transfected into cells using Xtreme gene HP reagent (Roche, Indianapolis, IN).

ELISA Assays

The concentration of TGF-β1 protein content in peritoneal fluids was determined by an ELISA kit specific for rat TGF-β1 (rat0736, Andygene, Beijing, China). Peritoneal fluids were

centrifuged at 4000 g for 15 min. The total protein content of peritoneal fluid supernatants was determined using the Qubit Protein Assay (Invitrogen, Carlsbad, CA, USA). Aliquots were stored at -80°C until assayed. An equal volume of total protein from each preparation was subjected to ELISA in duplicate. The results are reported as mean \pm standard error of the mean (SEM).

Electrophysiology

Whole-cell chloride currents were measured using the patch clamp technique with an EPC-7 patch-clamp amplifier (HEKA, Lambrecht/Pfalz, Germany) as previously described[2]. The standard pipette solution contained 70 mM N-methyl-D-glucamine chloride (NMDG-Cl), 1.2 mM MgCl_2 , 10 mM HEPES, 1 mM EGTA, 140 mM D-mannitol, and 2 mM ATP. The external isotonic bath solution contained 70mM NaCl, 0.5 mM MgCl_2 , 2 mM CaCl_2 , 10 mM HEPES, and 140 mM D-mannitol. The 47% hypotonic bath solution was obtained by omitting D-mannitol from the solution, giving an osmolarity of 160 mosmol/L. The 47% hypertonic solution was obtained by adding D-mannitol to the isotonic solution, giving an osmolarity of 440 mosmol/L.

Cell Volume Measurements

Cell volume was measured as described previously[3]. Time-lapse images of cells transfected with pGPU6/GFP-MDR1 shRNA vector were taken using a fluorescence microscope (IX-71; Olympus, Tokyo, Japan) equipped with a CCD camera (SC35; Olympus). The acquisition of cell images was controlled by the Image-Pro Plus software (Media Cybernetics, Silver Springs, USA). Cell volume was calculated using the equations of $V = 4/3 \times S \times (S/\pi)^{1/2}$; where S is the area (μm^2). The level of regulatory volume decrease (RVD) was calculated using the equation: $\text{RVD} (\%) = (V_{\text{max}} - V_{\text{min}}) \div (V_{\text{max}} - V_0) \times 100\%$, where V_0 is the cell volume in isotonic solution before hypotonic shock, V_{max} is the peak volume in hypotonic solutions, and V_{min} is the volume before returning to isotonic solution. The percentage block of RVD by an inhibitor was calculated using the equation, inhibition of RVD (%) = $(\text{RVD}_{\text{ctrl}} - \text{RVD}_t) \div \text{RVD}_{\text{ctrl}} \times 100\%$, where RVD_{ctrl} is the RVD in control cells and RVD_t is the RVD of treated cells.

Cell Migration Assay

In vitro wound-scratch experiments were performed to assess migratory potential as

previously described[4]. Briefly, cells were seeded in 24-well plates and allowed to grow to confluence. Confluent monolayers were scratched with a 200- μ l pipette tip. The cells were then cultured for 48 h. The images were recorded using a photomicroscope (Leica DFC950 camera; Leica Microsystems, Wetzlar, Germany) and cell migration was quantitated using Scion Image software (beta 4.0.2, Scion, Frederick, MD).

Cell Proliferation

Proliferation of primary cultured cells was assessed by monitoring peritoneal or adhesive tissues using the IX-71 microscope. Cell number was calculated by Image-Pro Plus. Proliferation of subcultured cells was measured using a Cell Proliferation Reagent Kit (CCK-8, Dojindom, Kumamoto, Japan). Fibroblasts were seeded in 96-well plates at 2,000 cells per well. Cell proliferation was assessed at 0, 1, 3, 5, and 7 days after cell seeding following the manufacturer's protocol. The absorbance at 450 nm was measured using an automated microplate reader (type Elx800, Bio-Tek Instruments, Winooski, USA).

Statistical analysis

Statistical analysis was performed using IBM SPSS Statistics 22.0 (SPSS Inc., Chicago, Illinois). Differences in the numbers of animals without adhesions in the different treatment groups were evaluated using a Mann-Whitney U test. Spearman's correlation test and crosstabs ranking difference and Kruskal-Wallis were used when necessary. A t-test was used to determine differences between two independent populations. A value of $P < 0.05$ was considered significant.

Supplemental Tables

Supplemental Table 1. The effect of ascites reinfusion on peritoneal adhesions

| Group | n | Grade of adhesion (case) | | | | | Average grade | Rate of adhesion [case (%)] |
|----------------|---|--------------------------|---|---|---|---|---------------|-----------------------------|
| | | 0 | 1 | 2 | 3 | 4 | | |
| Normal ascites | 6 | 0 | 3 | 1 | 1 | 1 | 2 | 6 (100) |
| Ascites from | 6 | 0 | 0 | 0 | 3 | 3 | 3.5 | 6 (100) |

peritoneal
adhesion mice*

* $P < 0.05$ as compared to the normal ascites group (Mann-Whitney U test).

Supplemental Table 2. The effect of TGF- β 1 intraperitoneal injection on peritoneal adhesion

| Group | n | Grade of adhesion (case) | | | | | Average grade | Rate of adhesion [case (%)] |
|-----------------|---|--------------------------|---|---|---|---|---------------|--------------------------------|
| | | 0 | 1 | 2 | 3 | 4 | | |
| PBS | 6 | 1 | 2 | 2 | 0 | 1 | 1.7 | 5 (83) |
| TGF- β 1* | 6 | 0 | 0 | 1 | 1 | 4 | 3.5 | 6 (100) |

* $P < 0.05$ as compared to the PBS group (Mann-Whitney U test).

Supplemental Table 3. The effect of tariquidar on peritoneal adhesion

| Group | n | Grade of adhesion(case) | | | | | Average grade | Rate of adhesion [case(%)] |
|------------|---|-------------------------|---|---|---|---|---------------|-------------------------------|
| | | 0 | 1 | 2 | 3 | 4 | | |
| Tariquidar | 7 | 1 | 1 | 0 | 3 | 2 | 2.6 | 6(86) |
| Control | 7 | 0 | 1 | 1 | 2 | 3 | 3 | 7(100) |

$P > 0.05$ as compared to the control group (Mann-Whitney U test)

Supplemental Table 4. The effect of verapamil on peritoneal adhesion

| Group | n | Grade of adhesion(case) | | | | | Average grade | Rate of adhesion [case(%)] |
|---------|----|-------------------------|---|---|---|---|---------------|-------------------------------|
| | | 0 | 1 | 2 | 3 | 4 | | |
| Control | 10 | 0 | 0 | 0 | 8 | 2 | 3.20 | 10(100) |
| 5mg/kg | 10 | 0 | 3 | 3 | 2 | 2 | 2.30 | 10(100) |
| 10mg/kg | 10 | 0 | 2 | 5 | 2 | 1 | 2.20 | 10(100) |
| 15mg/kg | 10 | 1 | 5 | 3 | 1 | 0 | 1.40 | 9(90) |
| 30mg/kg | 9 | 5 | 2 | 1 | 1 | 0 | 0.78 | 4(44) |

Crosstabs, Chi-square test $P < 0.01$; Spearman's correlation analysis, $r = -0.53$, $P < 0.01$.

Supplemental Refences

1. Pichler A, Zelcer N, Prior JL, Kuil AJ, Piwnica-Worms D. In vivo RNA interference-mediated ablation of MDR1 P-glycoprotein. *Clin Cancer Res.* 2005; 11: 4487-94.
2. Chen L, Wang L, Zhu L, Nie S, Zhang J, Zhong P, et al. Cell cycle-dependent expression of volume-activated chloride currents in nasopharyngeal carcinoma cells. *Am J Physiol Cell Physiol.* 2002; 283: C1313-23.
3. Mao JW, Wang LW, Jacob T, Sun XR, Li H, Zhu LY, et al. Involvement of regulatory volume decrease in the migration of nasopharyngeal carcinoma cells. *Cell Res.* 2005; 15: 371-8.
4. Preet A, Ganju RK, Groopman JE. Delta9-Tetrahydrocannabinol inhibits epithelial growth factor-induced lung cancer cell migration in vitro as well as its growth and metastasis in vivo. *Oncogene.* 2008; 27: 339-46.

Supplemental Figure Legends

Figure S1. Real-time Quantitative RT-PCR Analysis of Expression of Genes Related to Cell Migration and Proliferation in Human NFB and AFB.

(A) Representative real-time PCR curves for MDR1 expression. (B) Relative quantitative analysis of mRNA levels in NFB and AFB. MDR1 mRNA expression is significantly up-regulated in cultured human AFB. Values are given as means \pm SEM.

Figure S2. Knockdown of P-gp Expression by Rat Intraperitoneal Injection of MDR1 siRNAs Formulated with in vivo-jetPEI.

(A) Immunohistochemical detection of P-gp in rat colon following intraperitoneal injection of formulated MDR1 siRNAs (Si-MDR1) or control siRNAs (Si-NC). (B) Average optical density (AOD) values of P-gp-positive cells. Values are expressed as mean \pm SEM ($n = 3$). (C) Relative quantitative analysis of mRNA levels in rat colons following Si-MDR1 or Si-NC intraperitoneal injection. P-gp is highly expressed in rat intestinal mucosal epithelium and the intraperitoneal injection of MDR1 siRNAs significantly down-regulated P-gp mRNA and protein expression.

Figure S3. Effects of TGF- β 1 on P-gp Expression of Rat NFB.

(A) Western blotting analysis of P-gp expression in rat NFB treated with different concentrations of TGF- β 1 for 24 h. NFB were subjected to serum starvation (0.5% FCS) during treatment time. A low concentration of TGF- β 1 up-regulated P-gp expression, which peaked at 4 ng/ml. (B) Effects of interference of TGF- β /Smad signaling pathway and histone acetylation on MDR1 mRNA expression of rat NFB. Cells were cultured at a low serum concentration (0.5%) for 24 h. Then cells were treated with 4ng/ml TGF- β 1 for 4h followed by 10 μ M TGF- β type I receptor (T β RI) inhibitor SB431542 for 30min or 20 μ M histone acetyltransferase CBP/p300 inhibitor C646 for 1 h. For histone deacetylase (HDAC) inhibitor LBH589, cells were treated for 24 h in medium with low serum and 500 nM of the drug. LBH589 and TGF- β 1 increased MDR1 mRNA expression and the increased activity induced by TGF- β 1 was abolished by SB431542 and C646.

Figure S4. Volume-activated Cl⁻ Current in Rat Adhesion Fibroblasts.

(A) Typical current traces of AFB recorded under isotonic bath conditions (ISO) and at the peak of hypotonic response (Hypo) are shown. Voltage was held at 0 mV and then stepped to \pm 40, 0, and \pm 80 mV. Current-voltage (*I-V*) relationships are presented (right). (B) Anion permeability of the volume-activated Cl⁻ channel in AFB. Permeability ratios (P_x, P_{Cl}) of various anions (X^-) relative to that of Cl⁻ were calculated using the modified Goldman-Hodgkin-Katz equation, $P_x/P_{Cl} = \{ [Cl^-]_i^n \exp(-\Delta V_{rev} F/RT) - [Cl^-]_o \} / [X^-]_o$. Data represent mean \pm SE (n = 3). (C) The current-voltage (*I-V*) curve revealed that gluconate shifted the reversal potential at -22.85 ± 3.5 mV. (D) Down-regulation of CIC-3 by Si-CIC-3 transfection inhibited volume-activated Cl⁻ current. (E) Inhibition of regulatory volume decrease (RVD) by Si-CIC-3 transfection.

Figure S5. Silencing of MDR1 Expression by sh-MDR1 Transfection in Rat AFB.

AFB cells were transfected with pGPU6/GFP-MDR1 shRNA (sh-MDR1) or pGPU6/GFP sh-NC (sh-NC) plasmids for 48 h. Cells were then fixed with paraformaldehyde and incubated with anti-P-gp antibody and Alexa Fluor 555-conjugated secondary antibody. (A) Cells successfully transfected with sh-MDR1 (green) showed an obvious decrease in P-gp staining (red). Relative quantitative analysis is shown in (B). Data are presented as mean \pm SEM.

Figure S6. P-gp co-localized with CIC-3 at in migrating AFB cells.

P-gp and CIC-3 were detected by immunofluorescence with anti-P-gp and CIC-3 antibodies and Alexa Fluor 488 and 555-conjugated secondary antibodies, respectively. Confocal z-sections were obtained every 0.35 μm . (Left panels) 3D-reconstruction of subcellular co-localization of P-gp and CIC-3 at lamellipodia. The Pearson coefficient was 0.68 ± 0.02 (mean \pm SEM, n=5). Lamellipodia are shown by pink rectangles. (Right panels) The crosshairs and arrows depict co-localization of P-gp and CIC-3 at the rear of the migrating cell. The Pearson coefficient was 0.76 ± 0.06 (mean \pm SEM, n=4).

Figure S7. Effect of TGF- β 1 Treatment on the Amount of Membranous CIC-3.

(A) Representative western blot probed for CIC-3 in membrane and cytoplasmic fractions. (B) Densitometric analysis revealed that TGF- β 1 stimulation significantly increased the amount of CIC-3 on the membrane surface and decreased the amount of cytoplasmic CIC-3.

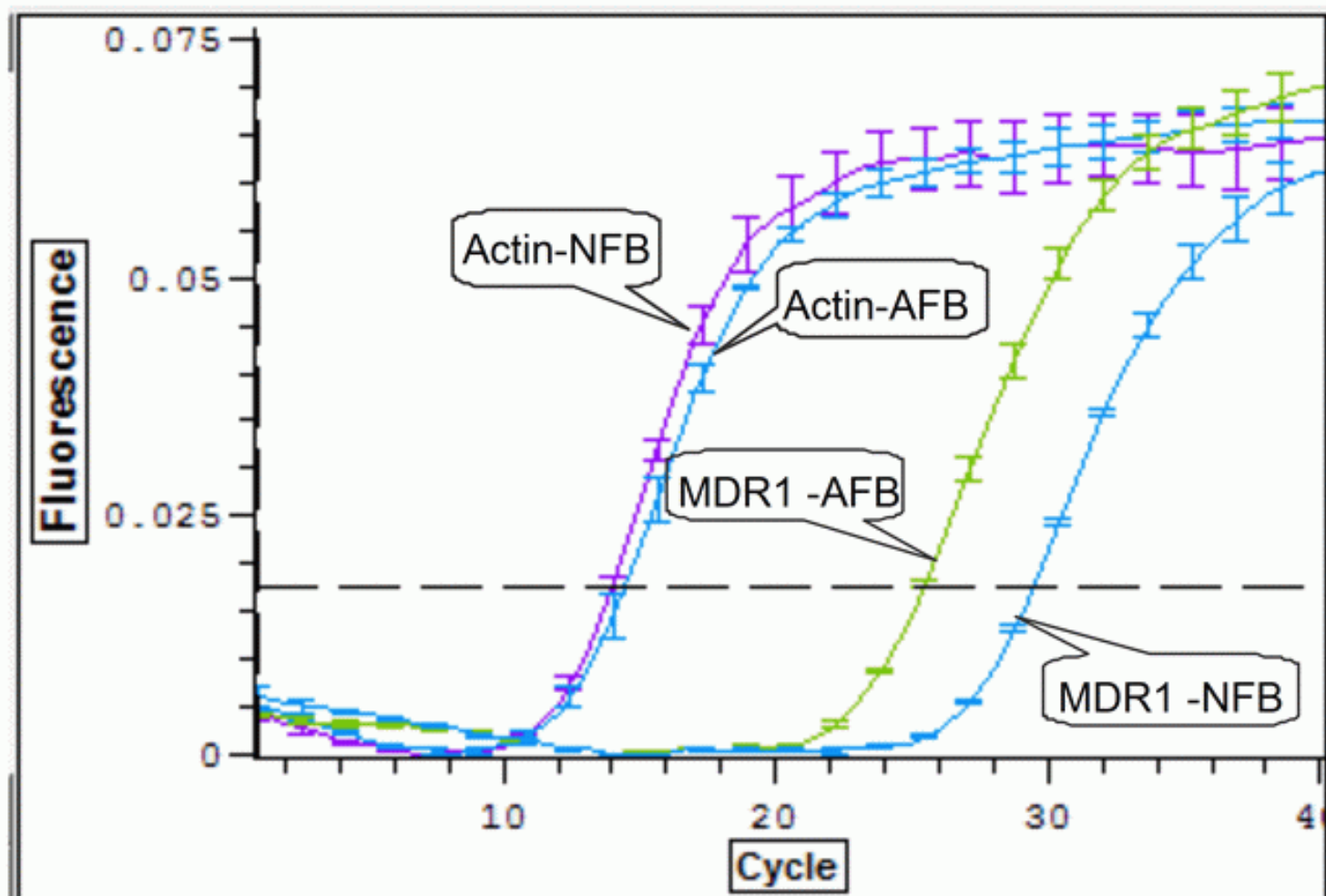
Figure S8. Effects of silencing P-gp and CIC-3 expression.

Representative Western blot (upper) and densitometric analysis (lower) revealed that silencing P-gp expression did not effect CIC-3 expression. However, silencing of CIC-3 expression significantly down-regulated P-gp expression.

Figure S9. Effects of Inhibitors of P-gp Transporter on the Formation of Peritoneal Adhesions.

The P-gp transporter inhibitor tariquidar (8 mg/kg) had no effect on the formation of peritoneal adhesions induced by peritoneal injury to rats. (B) The P-gp transporter and volume-activated Cl^- current inhibitor verapamil significantly decreased the formation of peritoneal adhesions in a dose-dependent manner, with an IC_{50} value of 11.41 mg/kg.

A



B

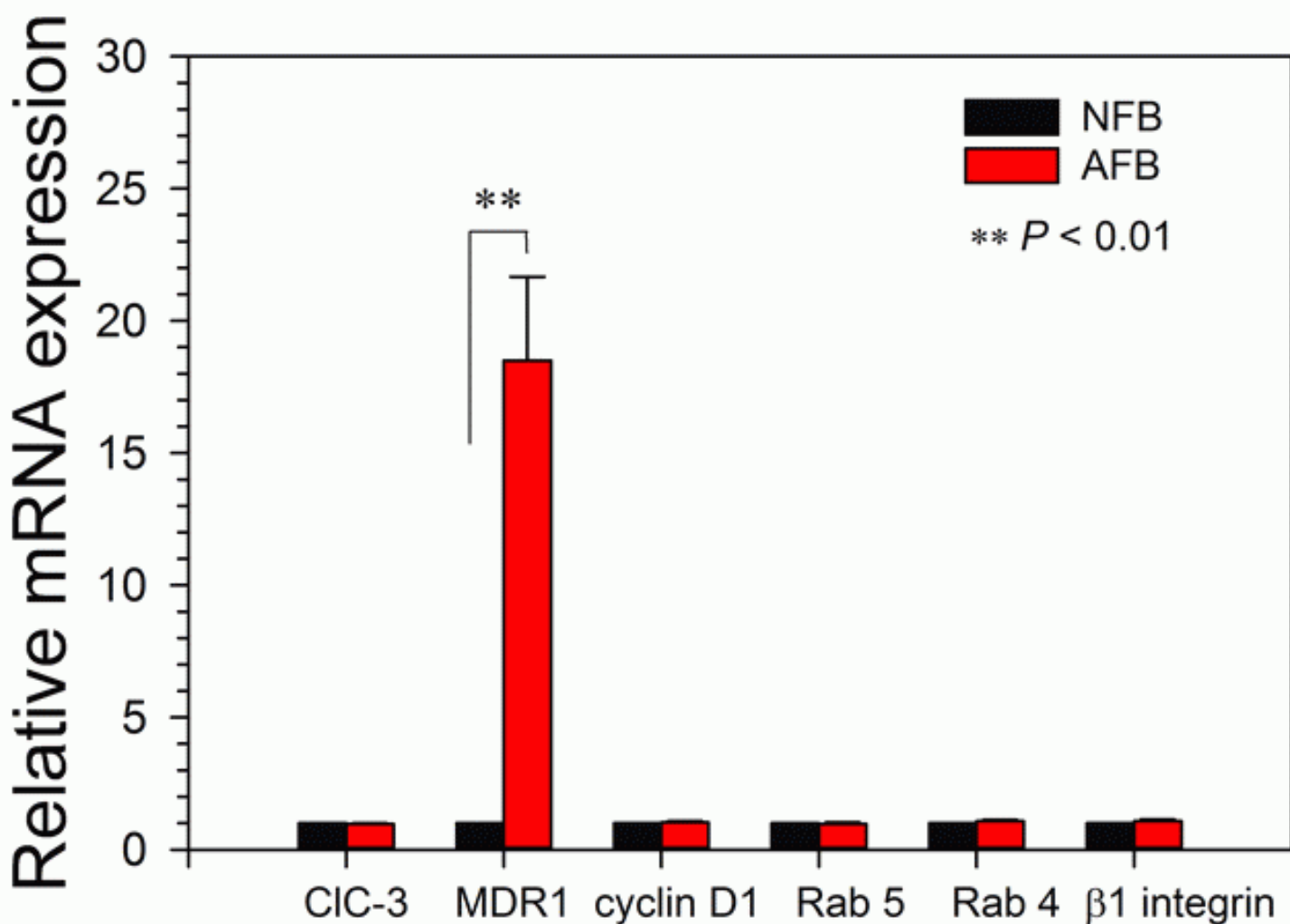


Figure S1

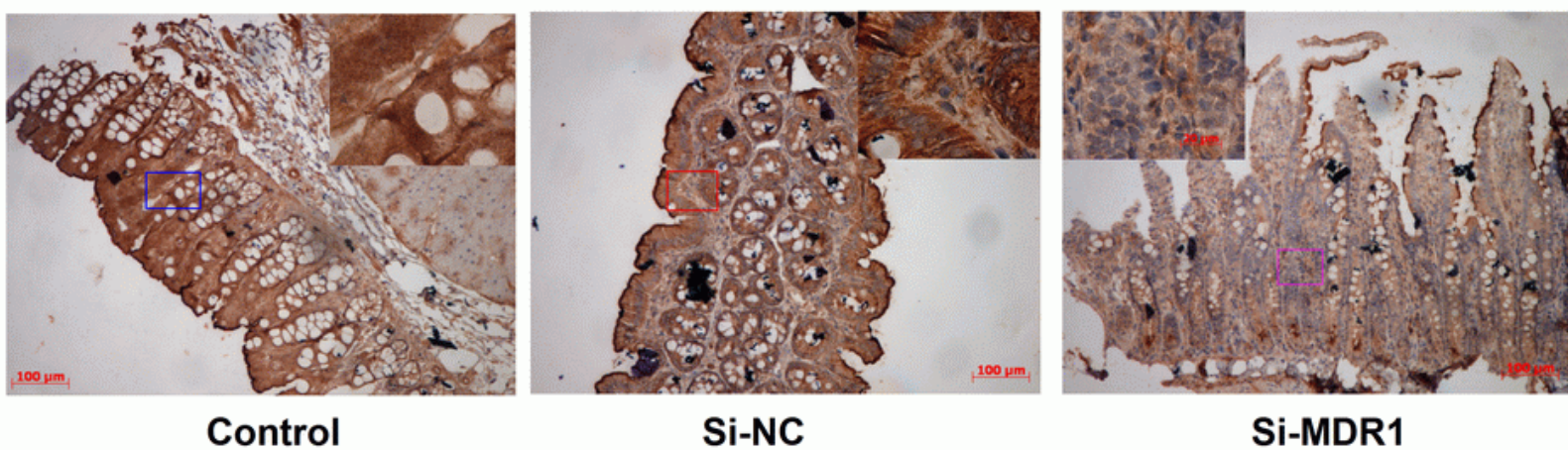
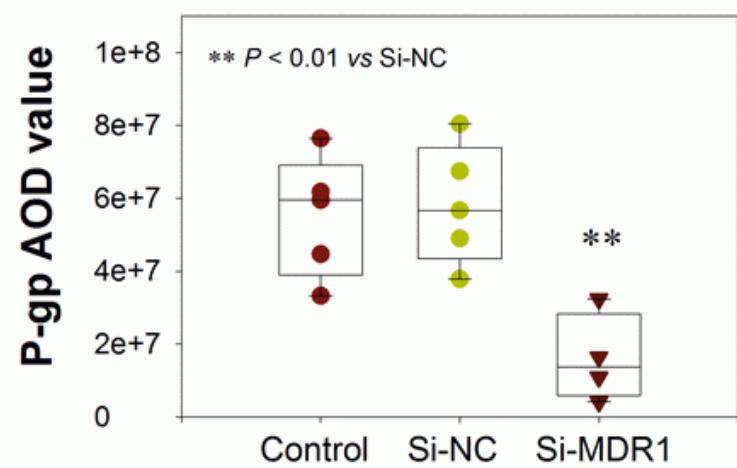
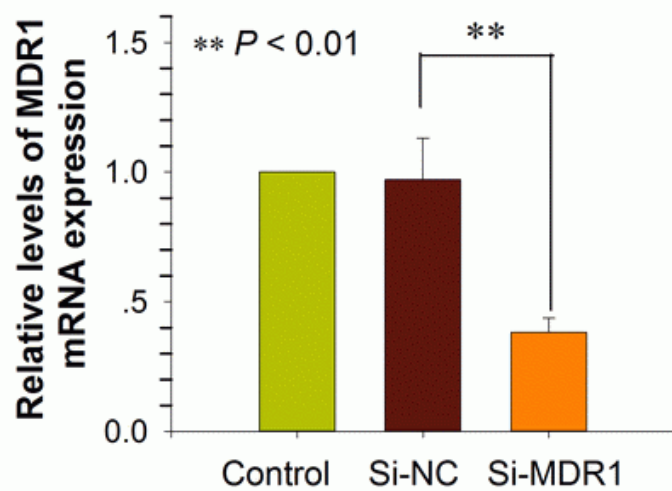
A**B****C**

Figure S2

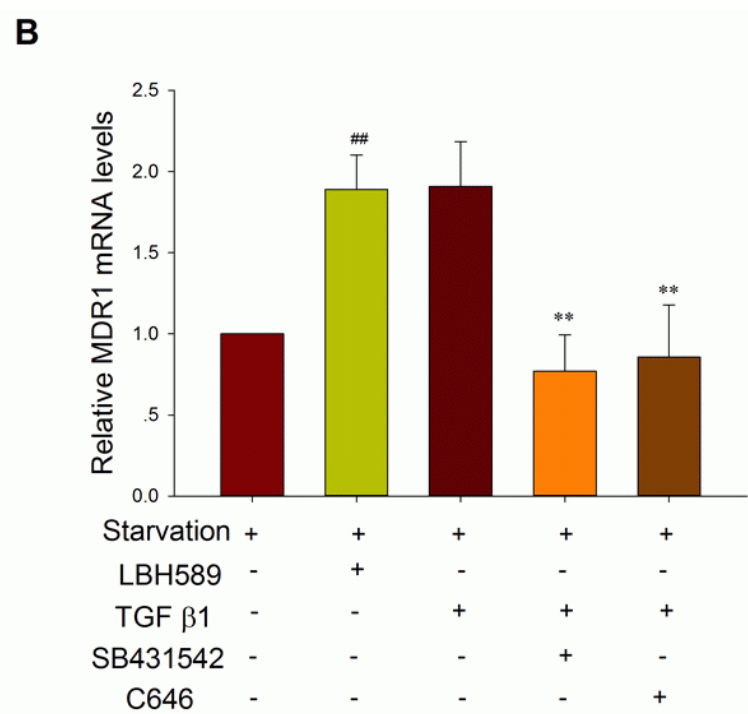
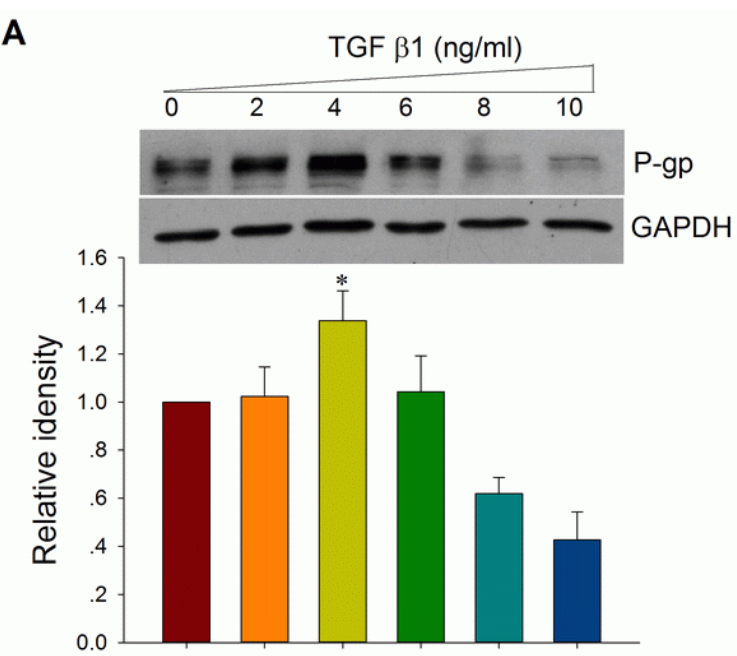


Figure S3

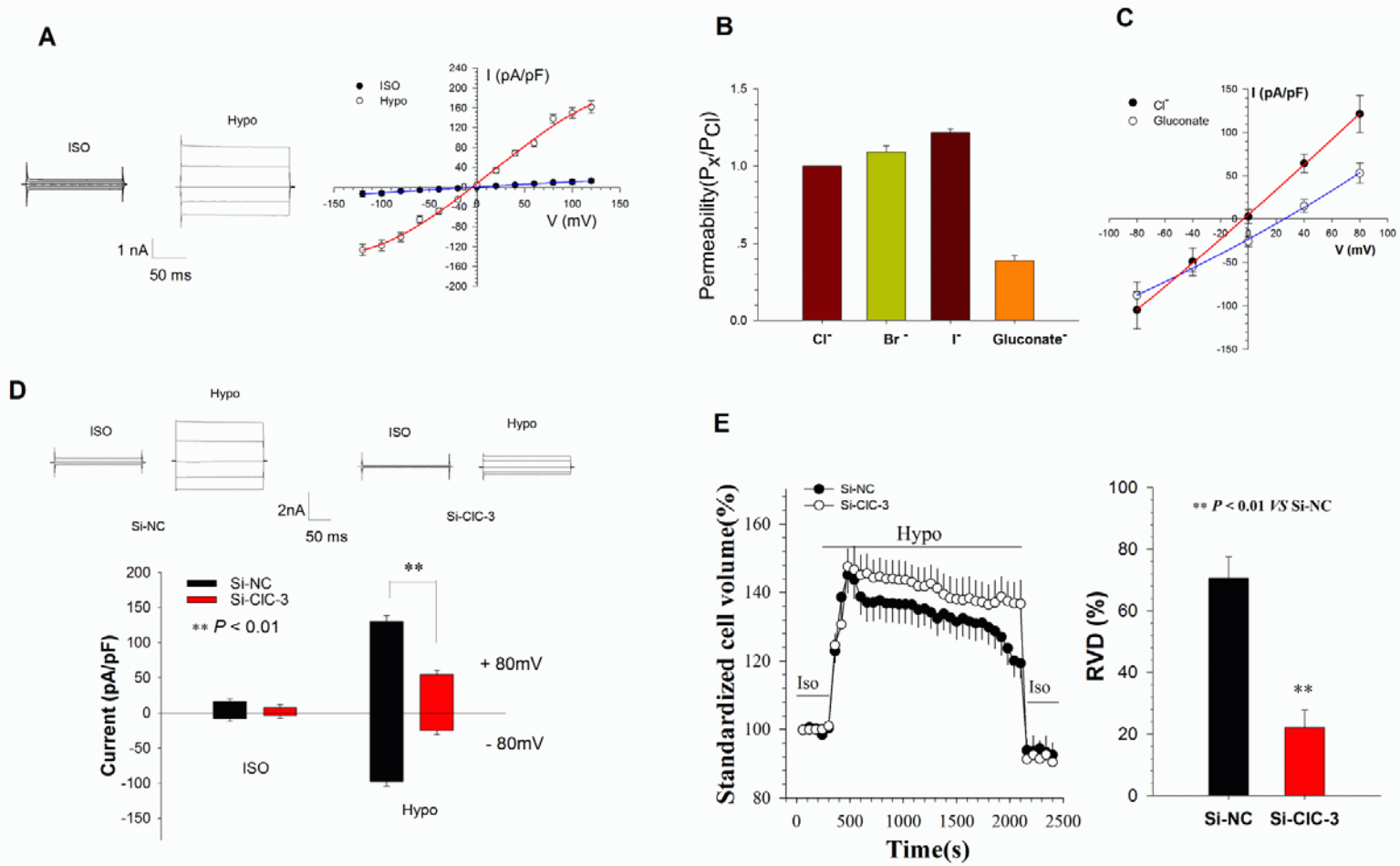


Figure S4

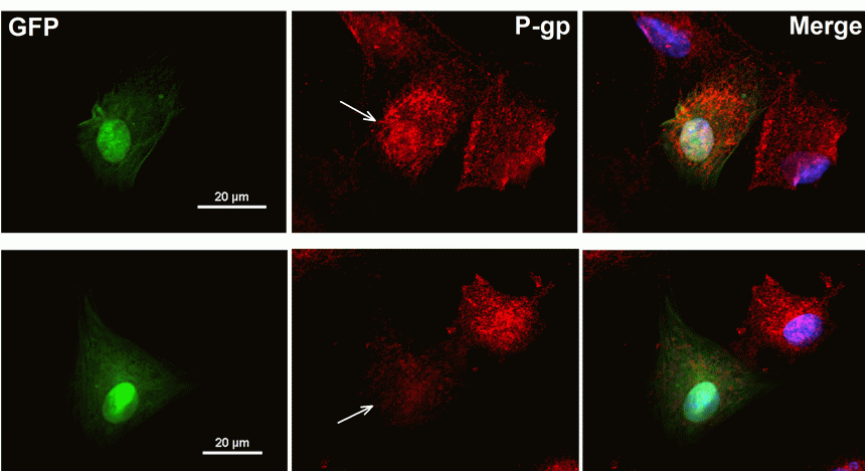
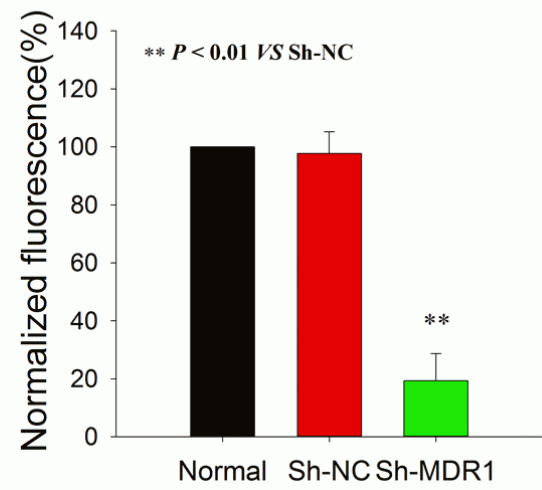
A**B**

Figure S5

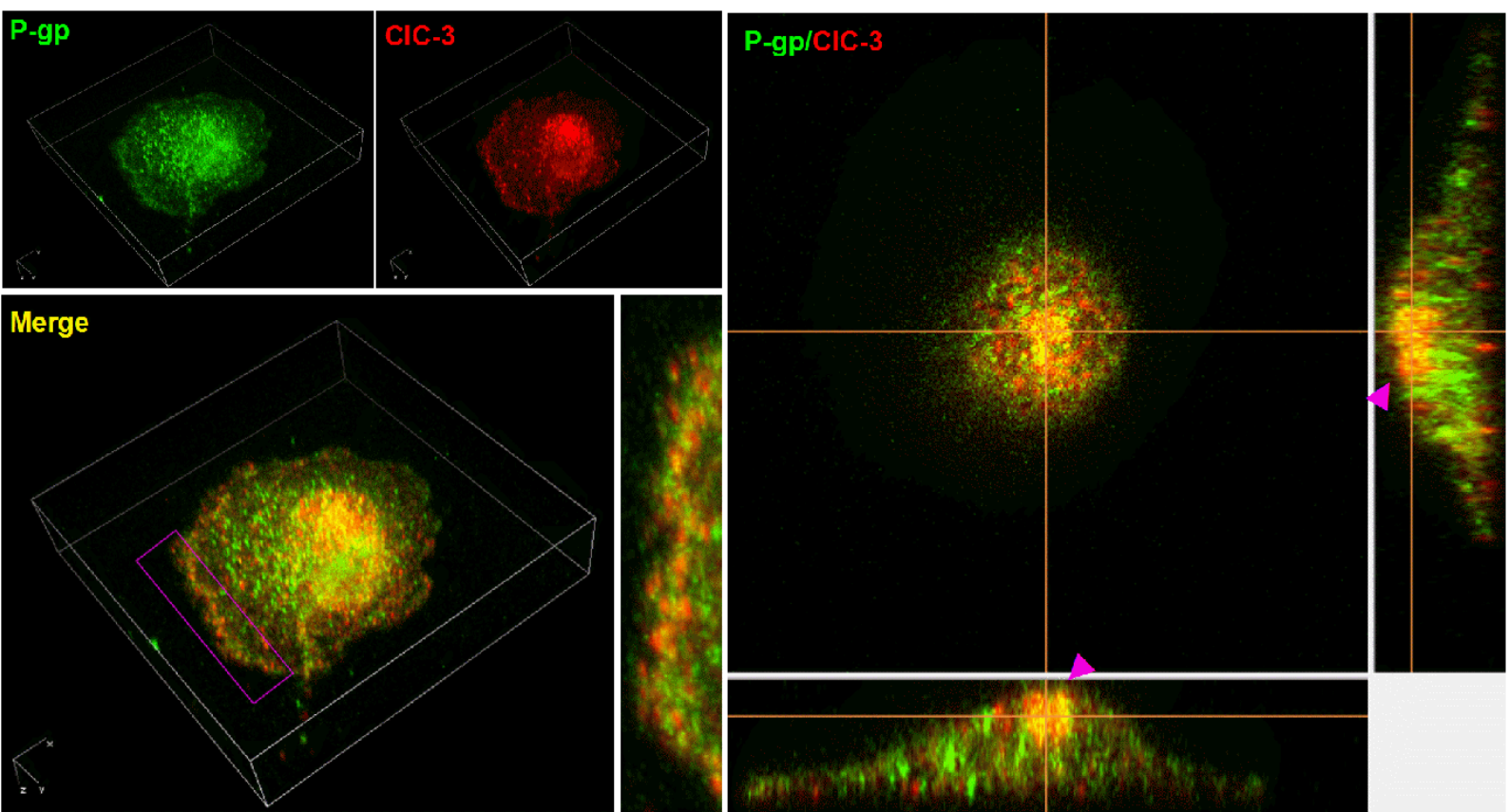


Figure S6

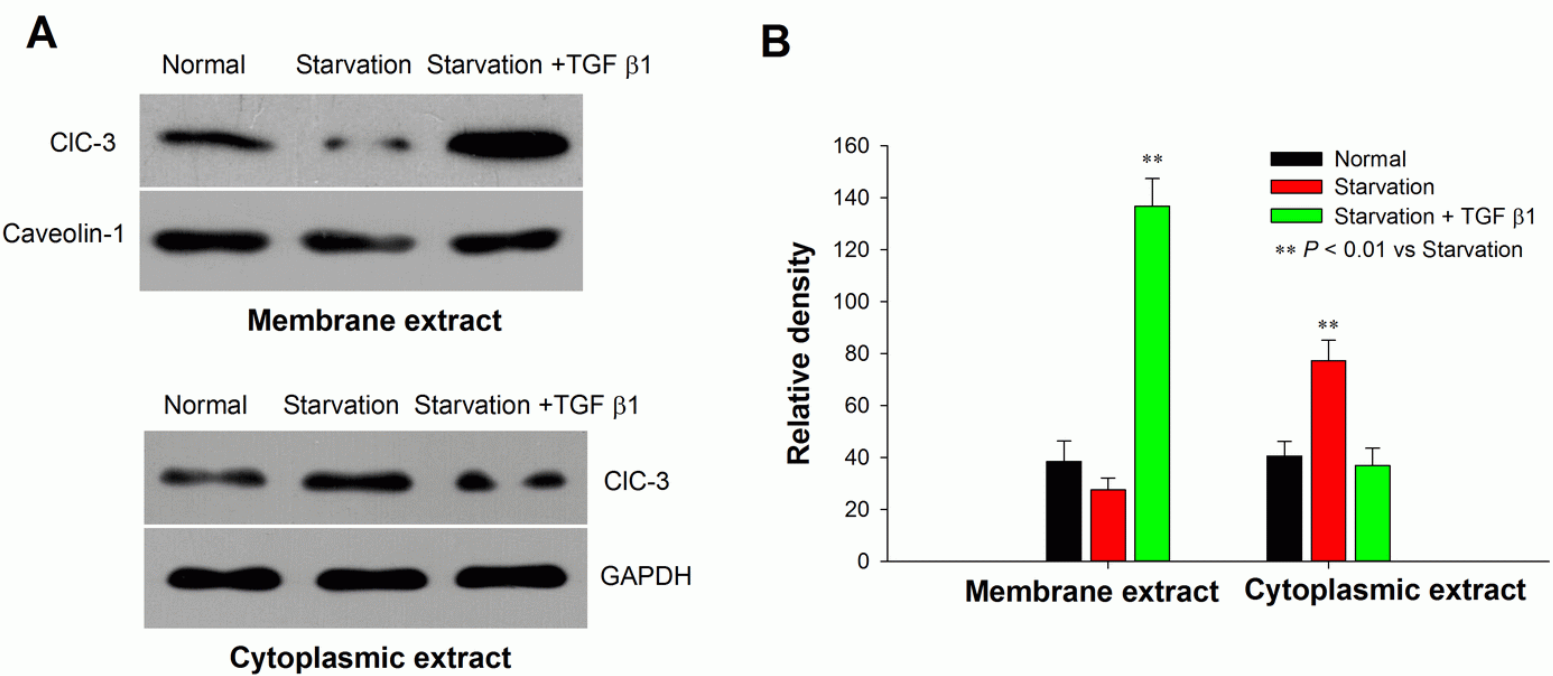


Figure S7

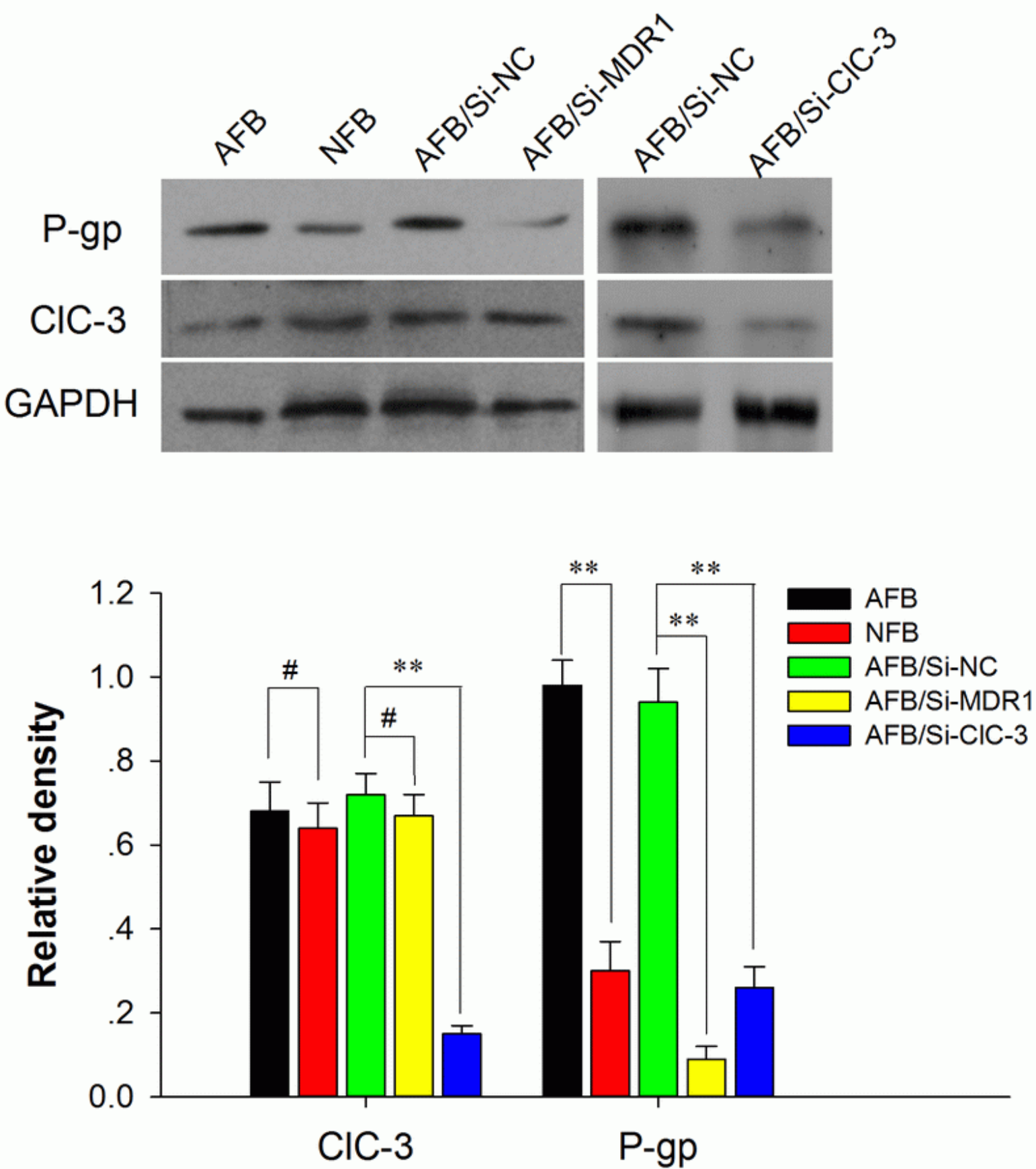


Figure S8

A



Tariquidar

Control

B



Control

5 mg/kg

15 mg/kg

30 mg/kg

Figure S9